# Energy & Environmental Science

Accepted Manuscript






ROYAL SOCIETY OF CHEMISTRY

www.rsc.org/ees

# Perovskite photovoltachromic cells for building integration

*Alessandro Cannavale*[a]° *and Giles Eperon*[b]°, *Pierluigi Cossari*[a], *Antonio Abate*[b]*, *Henry J. Snaith*[b]* *and Giuseppe Gigli*[a,c]*

[a] *Dipartimento di Matematica e Fisica "E. de Giorgi", Università del Salento, Via Monteroni, 73100, Lecce (Italy)*

[b] *Department of Physics, University of Oxford, Oxford, Parks Road,OX1 3PU, U.K.*

[c] *Istituto di Nanotecnologia, CNR-Nanotec, Via Arnesano 16, 73100 Lecce, Italy*

° *These authors contributed equally to the work*

**Corresponding Authors:* AA antonioabate83@gmail.com; HJS h.snaith1@physics.ox.ac.uk; GG giuseppe.gigli@unisalento.it

**Keywords**: photovoltaic, solar cells, photovoltachromic, perovskite, solid-state electrolyte, polymeric electrolyte, building integration, smart windows.

**Abstract**

Photovoltachromic devices combine photovoltaic and electrochromic behaviours to enable adjustable transparency glazing, where the photovoltaic component supplies the power to drive the colouration. Such stand-alone, self-powered devices are of commercial interest for integration into windows and surfaces of buildings and vehicles. Here, we report for the first time a perovskite-based photovoltachromic device with self-adaptive transparency. This multifunctional device is capable of producing electric power by solar energy conversion as well as undergoing a chromic transition from neutral-colour semi-transparent to dark blue-tinted when irradiated by solar light, without any additional external bias. The combination of a semi-transparent perovskite photovoltaic and solid-state electrochromic cells enables full solid-state photovoltachromic devices with 26% (or 16%) average visible transmittance and 3.7% (or 5.5%) maximum light power conversion efficiency. Upon activating the self-tinting, the average visible transmittance drops to 8.4% (or 5.5%). These results represent a significant step towards the commercialization of photovoltachromic building envelopes.

## INTRODUCTION

In recent years, the energy market registered a growing demand of photovoltaic technologies (PVs) suitable for building integration.[1, 2] Conventional building envelopes, such as roofs and façades, could be replaced by PVs to make energy self-sufficient buildings. This challenging perspective is currently catalysing research activities aiming for new, aesthetically more appealing PVs. In particular, semi-transparent PV modules are strongly desired to replace a number of architectural elements commonly made with glass, such as windows and skylights.[3, 4] An ideal PV glazing should be neutral coloured and with a tunable level of transparency.[5] Actually, a large choice of colours and high transparency can be easily achieved with dye-sensitized and organic solar cells.[6-10] For example, Hinsch and co-workers demonstrated green-absorbing dye-sensitized modules with transmittance around 20% and solar power conversion efficiency (PCE) over 7%.[11] Furthermore, amorphous silicon modules have already appeared on the market of semi-transparent PVs a few years ago, though the red or brownish colouring has significantly limited their deployment.[5] More recently, perovskite solar cells[12] have been demonstrated as a new potential PV material for building integration.[13-18] Indeed, semi-transparent perovskite PVs have been reported with tunable visible transmittance between 10 and 50% and PCE spanning from 5 to 12%.[13, 16-18] Moreover, they can be prepared neutral coloured offering full flexibility to make aesthetically appealing building integrated PV.

In addition to mere aesthetic requirements, the transparency and the colouring of glazing building envelopes are critical to control the indoor thermal and visual comfort.[19, 20] A number of technologies have been proposed to deliver optically and thermally active building envelopes, which can adaptively modulate the solar radiation and thus the heat gain in buildings. For example, electrochromic windows, currently available on the market, can modulate their throughput of light and thereby heat by applying an external voltage bias.[21, 22] Bechinger and co-workers proposed self-powered electrochromic windows, namely photoelectrochromic cells (PECs), where the coloration process is self-generated and it adaptively changes with the external light condition.[23] In their original architecture,[24, 25] PECs were prepared by depositing the photoactive and the chromogenic electrodes on two glasses separated by a liquid electrolyte. The photoactive electrode was made by a dye-sensitized titanium dioxide layer and the chromogenic electrode with tungsten oxide ($WO_3$). To activate the colouration, photoexcited electrons are driven to accumulate into the $WO_3$, which becomes opaque adsorbing positively charged ions from the electrolyte solution.[23] In 2009, Wu and co-workers further advanced this field integrating PV and PEC technologies in a

single device, which is now termed a photovoltachromic cell (PVCC).[26] They demonstrated self-adaptive transparency up to 50% - only in the electrochromic central area - and maximum PCE below 1%. Although PVCCs are one of the most promising device concepts for building-integrated PV,[27-29] their current PCE is impractical for generating power on large-scale. Furthermore, they are prepared using liquid or gel electrolytes, which are a significant drawback for the processing and the durability.[30-32] To overcome this problem, several efforts have been devoted to the development of solid-state polymer electrolytes (SPEs) which could guarantee a good adhesion between the glass electrodes, high optical transparency, good mechanical properties, simple processability and, most importantly, no issues with leakage or evaporation over time.[33] Efficient SPEs have been prepared with complexes of lithium salts (LiX) and high molecular weight polyethylene oxide (PEO).[34, 35] PEO-LiX SPEs showed good ionic conductivity at room temperature, which makes them ideal candidates for application in solid-state PVCCs.

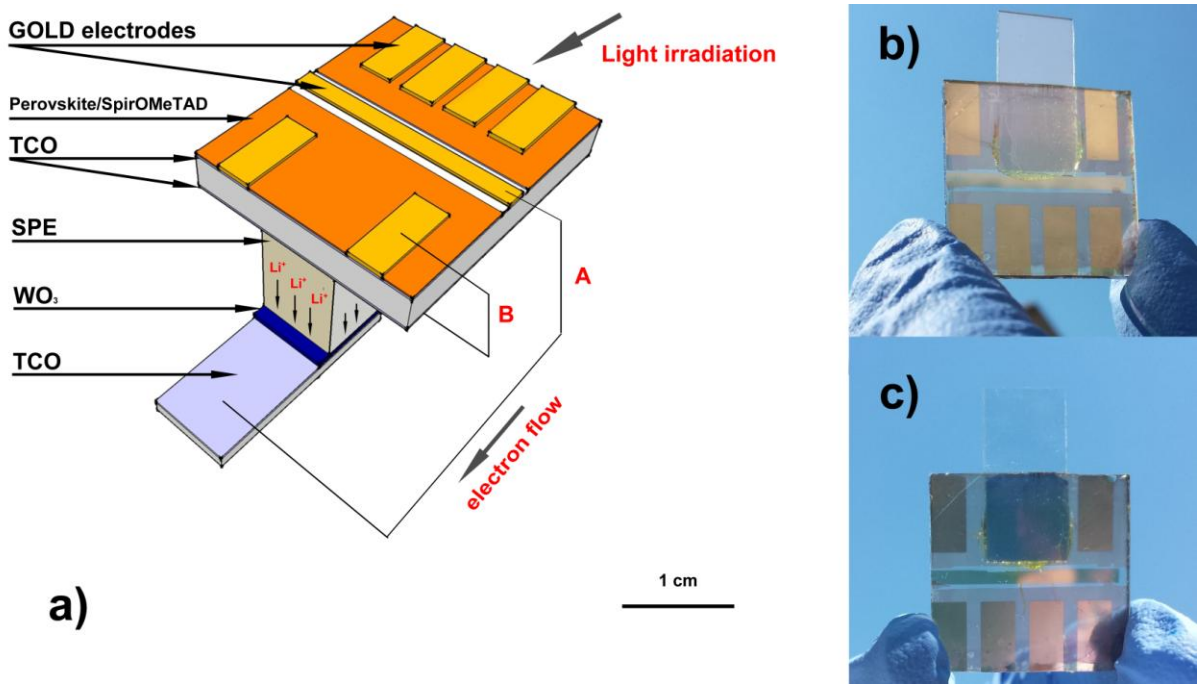


**Figure 1.** (a) Axonometric view of the photovoltachromic device. Two external circuits connect the photoanode to the electrochromic electrode (A) and the gold cathode to the secondary electrode of the electrochromic device (B). Pictures of the device in bleached (b) and coloured conditions (c) are shown on the right hand side. A schematic describing the colouration mechanism is reported in Supplementary information.

Here, we report a full solid-state perovskite PVCC with self-adaptive transparency and a maximum PCE over 5%. The device is realized by depositing the photovoltaic (PV) and the electrochromic (EC) layers on two separated glass sheets. In Figure 1a we report a scheme of this new device architecture. The top glass has both sides coated with transparent conductive oxides (TCO), which work as independent electrodes for the PV and the EC cells, while the bottom glass has only one side coated with TCO. The PV cell is made by a semi-transparent perovskite deposited on the top TCO glass. The EC layer is made by $WO_3$ deposited on the bottom TCO glass. A SPE prepared with PEO-LiX and polyethylene glycol (PEG) is used as a glue to laminate the two glasses and complete the EC cell. In Figure 1, we also show pictures of the prototype device with the EC active area completely bleached (b) and coloured (c). To activate the colouring, we connected the electrodes as described in Figure 1a and we exposed the device to solar light. Once the coloration has occurred, the PV cell can be used to generate useful power for an external circuit. In a photovoltachromic module, a switch can be used to direct the output of the PV cell as required to either the electrochromic or the external circuit.

## RESULTS AND DISCUSSION

Semi-transparent perovskite were prepared by controlling the film morphology in order to form an 'island-type' microstructure as described in our previous work.[13] We encouraged dewetting of the perovskite film from the TCO glass, causing it to form discrete micron-sized islands, indistinguishable to the naked eye. The islands are thick enough to be fully absorbing of incident light with energy above the bandgap of the perovskite semiconductor (~1.57eV).[12] The combination of fully absorbing islands and fully transparent regions results overall in a homogeneous-looking, semi-transparent and neutral-coloured perovskite film (see Figure 1b and c). We deposited the semi-transparent perovskite on TCO glass coated with a compact layer of $TiO_2$, which acts as electron collecting layer. Then, chemically doped spiro-OMeTAD (2,2',7,7'-Tetrakis-(N,N-di-4-methoxyphenylamino)-9,9'-spirobifluorene)[36-37] was used as hole collecting layer and gold top electrodes completed the PV cell defining the PV active area (see Figure 1a).

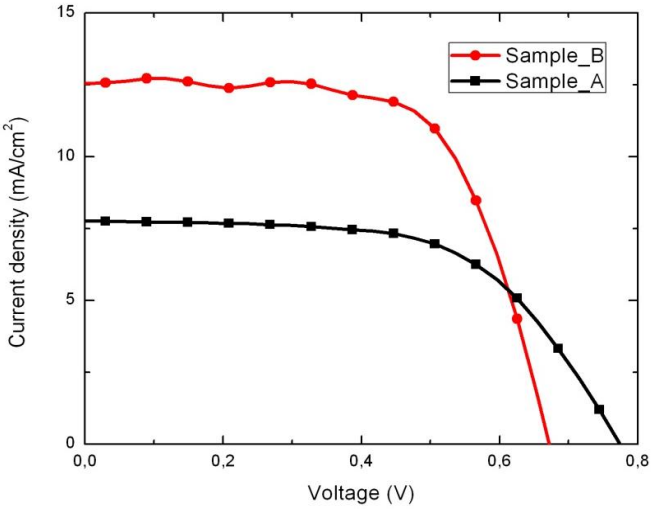


**Figure 2.** Current-voltage characteristics for the solar cell layers of the PVCC devices made with two different transparencies. Devices were measured under simulated 100 mW cm$^{-2}$ AM1.5 illumination as detailed in the Experimental section.

| | *$V_{oc}$ (V)* | *$J_{sc}$ (ma cm$^{-2}$)* | *FF* | *PCE (%)* | *AVT (%)* |
|---|---|---|---|---|---|
| **Sample A** | 0.77 | 7.8 | 0.59 | 3.7 | 26.1 |
| **Sample B** | 0.68 | 12.5 | 0.63 | 5.5 | 15.9 |

**Table 1**. Photovoltaic performance parameters of PVCCs with two different transparencies. Open circuit voltage ($V_{oc}$), short circuit current ($J_{sc}$) fill factor (FF) power conversion efficiency (PCE) and average visible transmittance (AVT).

We fabricated microstrucured perovskite films with two different surface coverages, meaning that the ratio of transparent and fully absorbing areas is changed, controlling the overall macroscopic transparency. In Figure 2, we show the current-voltage characteristics of the PV component of two PVCCs with different transparency (Sample A and B). The PV performance parameters and the average visible transmittance (AVT) are summarised in Table 1. AVT is defined as the mean transmittance between 370 nm and 740 nm; in the non-coloured state (bleached) it was measured as 26.1 and 15.9 % for the electrochromic areas of Sample A and B respectively. We note that here light is passing through the solar cell active layer plus the electrochromic cell, but not the gold electrodes. As already observed in our previous work,[13] the less transparent device (Sample B) displays significantly higher short-circuit current ($J_{sc}$) and an overall power conversion efficiency (PCE) of 5.5%, compared to the more transmissive device with PCE of 3.7%.

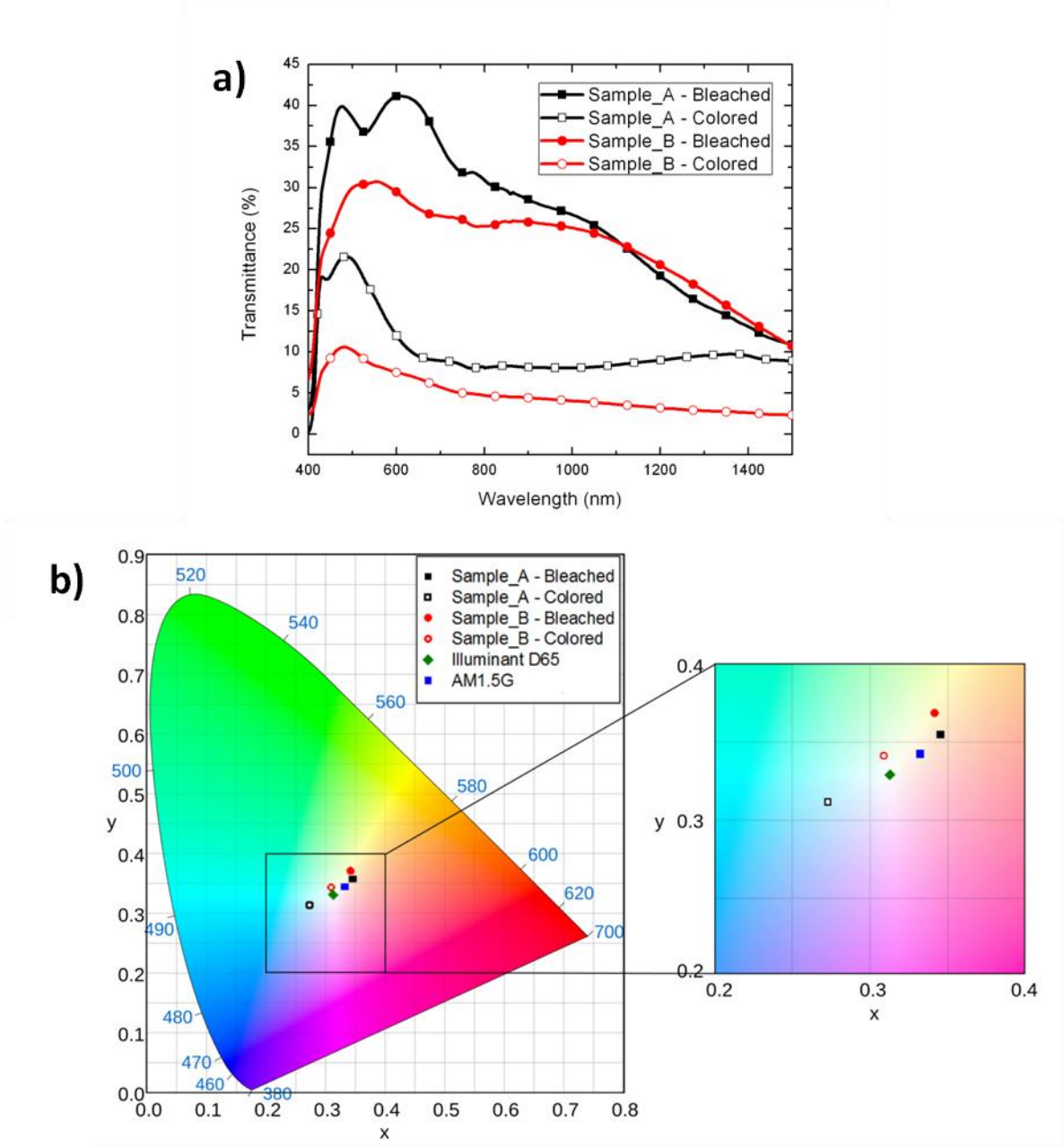


**Figure 3.** a) Transmittance spectra of complete PVCCs (Sample A and Sample B) in bleached and colored conditions in a range of wavelengths between 400 nm and 1500 nm. b) colour coordinates of the films with transmittance spectra shown in (a) under AM1.5 illumination, plotted on the CIE xy 1931 chromaticity diagram, and the enlarged central region. Colour coordinates of the D65 standard daylight illuminant and AM1.5 illumination are also shown.

In Figure 3a we show the bleached/coloured transmission spectra of the EC active area for Sample A and B. A maximum bleached/coloured modulation of 26 and 12% was observed at 635 nm for Sample A and B respectively. We also calculated the modulation averaged all over the visible spectra (370 – 740 nm), which was found to be about 18 and 10% for Sample

A and B respectively. Though these values are not yet comparable to what reported for electrochromic windows,[22] they are a remarkable result for self-powered devices. We also calculated the AVT after coloration for the electrochromic area of both devices; sample A changes from AVT of 26.1% (bleached) to 8.4% (coloured), and sample B from 15.9% to 5.5%. These are impressive changes in AVT, going from obviously transparent to obviously much more opaque. Clearly sample A, the more transparent perovskite sample, will make a more transparent window in the bleached state, but this is at the cost of photovoltaic performance.

In addition to modular transparency, neutral-colouring is particularly desired in glazing for building integration. To quantify the colour of the EC active area and the change it undergoes when transitioning from bleached to coloured, we calculated colour perception indices according to the CIE 1931 xy colour space standard.[36] In Figure 3b, we plot these colour coordinates of the transmission through the whole active region of the devices in both coloured and bleached states, compared to the reference daylight illuminant D65 and the AM1.5 spectrum. We observe that the PVCCs in the bleached state have good colour-neutrality, lying well within the central region of the chromaticity diagram, close to the AM1.5 spectrum. In the coloured state, both devices shift towards the blue side of the colour plot. Sample A demonstrates a more extreme change than sample B, as we would expect for the more absorbing sample. Despite shifting towards a bluer colour perception, both devices still exhibit colour perception close to the centre of the plot, and as such have good colour-neutrality, which make them ideal candidates for building integration.

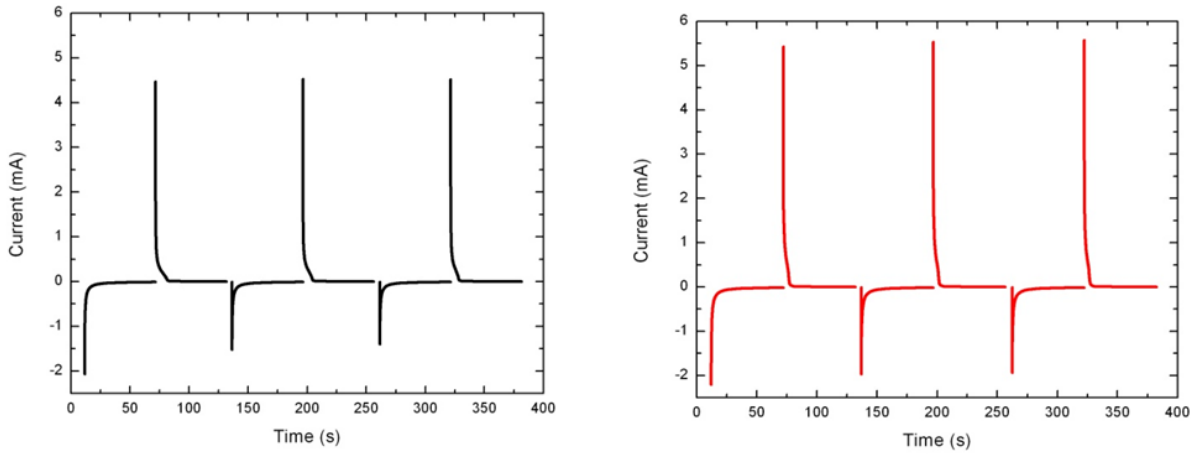


**Figure 4**. Chronoamperometric measurements for Sample A (left hand side) and Sample B (right hand side).

Figure 4 shows the chronoamperometric measurements of the EC cell in Sample A and Sample B. A voltage of – 0.6 V was applied to the electrodes of the EC part of the device. A prompt peak of current (about 2 mA) could be observed in both of the devices; such value decrease to roughly 30 μA in about 15-20 s, when the device reaches a stable coloration. Then, the bias was inverted and the bleaching took place with similar kinetics. We reported three complete cycles of colouring/bleaching showing that the coloration process is extremely fast and reproducible in both the samples.

We also calculated the electric power absorbed during the coloration process, using the same chronoamperometric curves in Figure 4. For Sample A we estimated an initial value of 2.7 mW $cm^{-2}$ (3.8mW $cm^{-2}$ for Sample B), which decays to zero within 15-20 s, when the colouration is completed. Therefore, the power produced by the PV component (3.7 and 5.5 mW $cm^{-2}$ for Sample A and B respectively) is thoroughly sufficient to drive the electrochromic component and it can be used in an external circuit after only 20 s, once the colouration is completed.

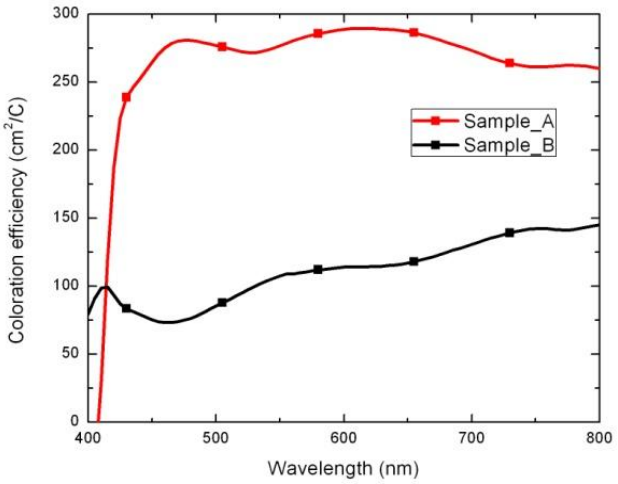


**Figure 5.** Coloration efficiency spectra of Sample A and Sample B.

To evaluate the quality of our EC cells we measured the colouration efficiency (CE), which is one of the most commonly used performance parameter.[24] To evaluate CE we used a well-known expression relating the efficiency with the optical density, which in turn depends on the transmittances of colored ($T_c$) and bleached states ($T_b$), and the insertion charge (Q), as follows:

$$CE = \frac{log\frac{T_b}{T_c}}{Q}$$

The plot for the electrochromic performance is shown in Figure 5. At a wavelength of 620 nm, the coloration efficiency was determined to be 289 $cm^2\ C^{-1}$ for Sample A and 114 $cm^2\ C^{-1}$ for Sample B. The higher performance observed in Sample A can be explained taking into account the higher transparency of device A in the bleached state and the lower amount of charge absorbed by Sample A during the colouration (3.3 compare to 4.4 mC for Sample B).

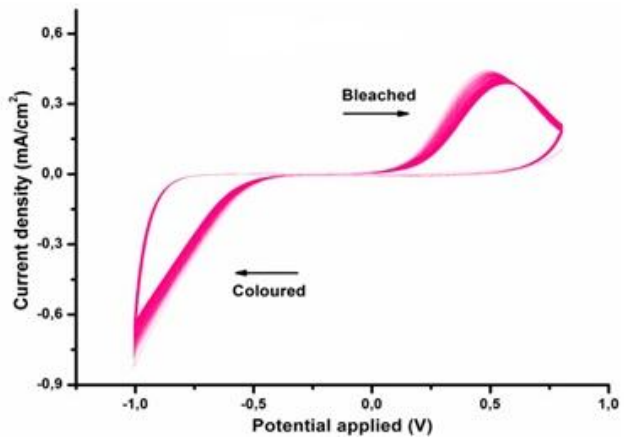


**Figure 6.** Cyclic voltammogram of the EC component of the PVCC showing 300 consecutive cycles.

Figure 6 shows the cyclic voltammogram (CV) of the EC component of the PVCC. The colouring and bleaching associated to $WO_3$ reduction and oxidation were observed by polarizing between -1 and 1 V. A stable current response was achieved after 50 cycles and no significant changes were observed up to 300 cycles, which indicates good electrochemical reversibility and stability within this time window. We highlight that the EC cell was assembled making use of our SPE (see Experimental section for a detailed formulation) as a glue to laminate the two glass electrodes and no additional sealing was used to protect the device from the humid air exposure (see Figure 1a and b). Further details on the device and the electrolyte stability are given in Supplementary information.

## EXPERIMENTAL

### Electron beam deposition

Tungsten oxide layers (550 nm thick $WO_3$) were deposited by electron beam deposition on ITO/glass substrates (VisionTech 12 Ω/□). The vacuum chamber was initially evacuated to $10^{-6}$ mbar, and then pure dry oxygen was admitted through a needle valve. The pressure was maintained at $10^{-4}$ mbar throughout the process. The deposition rate was about 1.5 Å $s^{-1}$. During the deposition process, the chamber reached a temperature of about 215 °C. High vacuum e-beam deposition was also performed to obtain a secondary ITO conductive layer on the FTO glass used for the photovoltaic purposes. More in detail, a 150 nm thick Indium tin oxide ($Sn:In_2O_3$) was used as a conductive layer in order to control the electrochromic functionality of the device. In this case, the vacuum chamber was initially evacuated to $10^{-7}$ mbar and then a pure dry oxygen flux was admitted through a needle valve. The pressure was maintained at $10^{-4}$ mbar throughout the deposition. The deposition rate was ~0.5 Å $s^{-1}$ and the substrate temperature was kept at 240°C during the process. Sheet resistance (20 Ω/□) was assessed by four-probe van der Pauw technique.

### Photovoltaic cell

Devices were fabricated on the fluorine-doped tin oxide side of the dual TCO coated glass. Initially FTO was removed from regions under the anode contact by etching the FTO with 2 M HCl and zinc powder. Substrates were then cleaned sequentially in hallmanex detergent, acetone, propan-2-ol and oxygen plasma. A ~50 nm hole-blocking layer of compact $TiO_2$ was deposited by spin-coating a mildly acidic solution of titanium isopropoxide in ethanol (350 ul in 5 ml ethanol with 0.013 M HCl) at 2000 rpm, and annealed at 500°C for 30 minutes.

Microstructured perovskite layers were deposited by spin-coating a non-stoichiometric precursor solution of methylammonium iodide and lead chlorine (3:1 molar ratio, final concentrations 0.88 M lead chloride, 2.64 M MAI) in anhydrous dimethylsulfoxide (DMSO). To make the more transmissive samples, spin-coating was carried out in ambient air at 2000 rpm for 45 s. These films were then annealed at 130°C for 20 minutes in ambient air. For the less transmissive samples, spin-coating was carried out in a nitrogen-filled glovebox at 2000 rpm for 45s. These films were then annealed at 130°C for 20 minutes in the glovebox. The hole-transporting layer was then deposited via spin-coating a 0.0788 M solution in chlorobenzene of 2,2',7,7'-tetrakis-(N,N-di-p-methoxyphenylamine)9,9'-spirobifluorene (spiro-OMeTAD), with additives of 0.0184 lithium bis(trifluoromethanesulfonyl)imide

(added in 0.61M acetonitrile solution) and 0.0659 M 4-tert-butylpyridine. Spin-coating was carried out at 2000 rpm in ambient air.

Gold electrodes were thermally evaporated under vacuum of ~$10^{-6}$ Torr, at a rate of ~0.1 nm $s^{-1}$ to complete the devices.

**Solid polymer electrolyte**

Anhydrous lithium iodide (LiI), poly(ethylene oxide) (PEO, Mw = 400,000), poly(ethylene glycol) (PEG, Mw = 400) and acetonitrile (ACN, anhydrous 99,8%) were purchased from Sigma-Aldrich and were used as received. All chemicals were stored in argon-filled glove box with < 1 ppm $H_2O$.

The PEO:PEG:LiI electrolyte was prepared with ether-oxygen to lithium [EO]:[Li+] molar ratio of 4:1, whereas the PEO:PEG weight ratio was fixed as 40:60. Homogeneous mixture of PEG and lithium salt was obtained by stirring the desired concentration of polymer and lithium salt for a period of at least 6 hours within a dry argon-filled preparative glove box. PEO was then dispersed in PEG/LiI system by adding anhydrous acetonitrile and stirred until it dissolved in the mixture. Finally, the residue solvent was evaporated at room temperature and the polymer electrolyte was dried under vacuum for 72 hours.

**Photovoltachromic device fabrication**

A small amount of SPE was spread on the $WO_3$ coated TCO glass and pressed on the second glass to reproduce the architecture reported in Figure 1a. Mechanical pressure and mild vacuum was applied for 1 hours to laminate the two glass electrodes and remove any residual of air in the electrolyte.

**Photovoltaic characterization**

The current density-voltage curves were measured (2400 Series SourceMeter, Keithley Instruments) under simulated AM 1.5 sunlight at 100 mW $cm^{-2}$ irradiance generated by an Abet Class AAB sun 2000 simulator, with the intensity calibrated with an NREL calibrated KG5 filtered Si reference cell. The mismatch factor was calculated to be less than 1%. The solar cells were masked with a metal aperture to define the active area of 0.2 $cm^2$. The current-voltage curves were collected scanning from forward bias to short circuit condition at 0.38 V $s^{-1}$. The impact of the hysteresis[37] on the estimated power conversion efficiency has been discussed for similar semi-transparent perovskite devices in our previous publication.[18]

**Electro-optical characterization**

Optical transmittance spectra of the short-circuited devices were observed by a VARIAN 5000 spectrophotometer in a wavelength range between 400 nm and 1500 nm. Full spectrum measurements were obtained by irradiating the short-circuited device using an array of seven white Luxeon LED (Cool White 6500 K, 7 LED 40 mm−1540 lm at 700 mA), operated by a Keithley source meter. During these measurements, the devices were connected as shown in Figure 1 using one photovoltaic pixel per time. Chronoamperometry measurements were collected with Autolab PGSTAT302N (Metrohm AG, the Netherlands) potentiostat.

**Electrochemical characterization**

Cyclic voltammetry and CA analysis of the EC device were performed on an Autolab PGSTAT 302N in the potential range of ±1V at a scan rate of 1mV s-1.

Electrochemical impedance spectroscopy (EIS) was carried out using an Autolab PGSTAT302N (Metrohm AG, the Netherlands) combined with a FRA32 frequency generator module by sweeping over 70 points in the frequency range from $10^{-1}$ – $10^{6}$ Hz with a root mean square (RMS) amplitude of 10 mV. The electrolytes with a diameter of 10 mm and a thickness of 50 µm were sandwiched between two stainless steel blocking electrodes separated by a Teflon ring. Impedance spectra were recorded after applying a coloration voltage of 1V for 10 min in order to reach a steady state. The ionic conductivity (σ) was calculated using the relation $\sigma = l/R_b A$, where $l$ is the thickness of the polymer electrolyte film, $A$ is the contact area between the electrolyte and the electrode, and $R_b$ is bulk resistance obtained from the intercept of the semicircle with the real axis of the Z' versus Z" Nyquist plot. The calculated ionic conductivity for the PEO-LiX SPE prepared in this work was 1.25 x $10^{-5}$ S $cm^{-1}$.

## CONCLUSION

In this work we reported for the first time perovskite PVCCs with self-adaptive transparency. The combination of a semi-transparent perovskite photovoltaic and SPE electrochromic enables full solid-state PVCC with 26% AVT and 3.7% maximum PCE (or 16% AVT and 5.5% maximum PCE), that switch to AVT of 8.4% (or 5.5%) upon self-activated tinting under illumination. This result represents a significant step towards the commercialization of building integrated PVCC, which will allow self-powered tinting windows, with the additional possibility of delivering external power. All of the key components of the system are relatively cheap and the fabrication is compatible with a lamination process, which is well-known to the glazing industry. Further advance of our device concept will come from replacing the gold with a semi-transparent top electrodes, which will allow to overlap the photovoltaic and the chromogenic active areas.

**ACKNOWLEDGMENT**

Dr. Vittorianna Tasco and Armando Genco are kindly acknowledged for technical support and beneficial discussions. GE is supported by the EPSRC and Oxford Photovoltaics though a CASE studentship. AA has received funding from the European Union's Seventh Framework Programme for research, technological development and demonstration under grant agreement no 291771.

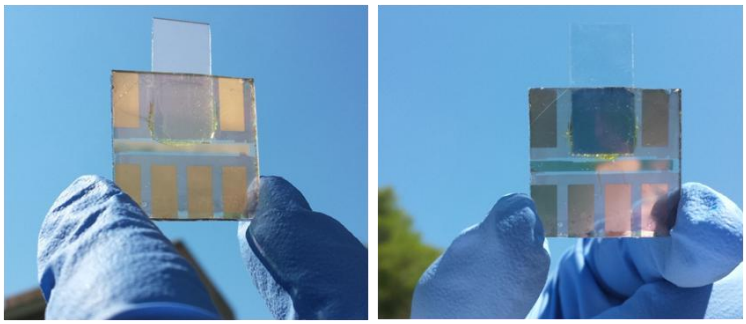

**Table of content pictures**

## REFERENCES


1. L. El Chaar and N. El Zein, *Renewable and Sustainable Energy Reviews*, 2011, 15, 2165-2175.
2. P. Heinstein, C. Ballif and L.-E. Perret-Aebi, *Green*, 2013, 3, 125-156.
3. B. P. Jelle, C. Breivik and H. D. Røkenes, *Solar Energy Materials and Solar Cells*, 2012, 100, 69-96.
4. C. Peng, Y. Huang and Z. Wu, *Energy and Buildings*, 2011, 43, 3592-3598.
5. P. Boyce, N. Eklund, S. Mangum, C. Saalfield and L. Tang, *Lighting research and Technology*, 1995, 27, 145-152.
6. B. O'regan and M. Grfitzeli, *Nature*, 1991, 353, 24.
7. C.-C. Chen, L. Dou, R. Zhu, C.-H. Chung, T.-B. Song, Y. B. Zheng, S. Hawks, G. Li, P. S. Weiss and Y. Yang, *Acs Nano*, 2012, 6, 7185-7190.
8. C. C. Chueh, S. C. Chien, H. L. Yip, J. F. Salinas, C. Z. Li, K. S. Chen, F. C. Chen, W. C. Chen and A. K. Y. Jen, *Advanced Energy Materials*, 2013, 3, 417-423.
9. C. Y. Chang, L. Zuo, H. L. Yip, C. Z. Li, Y. Li, C. S. Hsu, Y. J. Cheng, H. Chen and A. K. Y. Jen, *Advanced Energy Materials*, 2014, 4.
10. A. Yusoff, R. bin Mohd, S. J. Lee, F. K. Shneider, W. J. da Silva and J. Jang, *Advanced Energy Materials*, 2014, 4.
11. A. Hinsch, W. Veurman, H. Brandt, R. Loayza Aguirre, K. Bialecka and K. Flarup Jensen, *Progress in Photovoltaics: Research and Applications*, 2012, 20, 698-710.
12. M. M. Lee, J. Teuscher, T. Miyasaka, T. N. Murakami and H. J. Snaith, *Science*, 2012, 338, 643-647.
13. G. E. Eperon, V. M. Burlakov, A. Goriely and H. J. Snaith, *Acs Nano*, 2013, 8, 591-598.
14. P. Docampo, J. M. Ball, M. Darwich, G. E. Eperon and H. J. Snaith, *Nature communications*, 2013, 4.
15. J. You, Z. Hong, Y. M. Yang, Q. Chen, M. Cai, T.-B. Song, C.-C. Chen, S. Lu, Y. Liu and H. Zhou, *ACS Nano*, 2014, 8, 1674–1680.
16. C. Roldán-Carmona, O. Malinkiewicz, R. Betancur, G. Longo, C. Momblona, F. Jaramillo, L. Camacho and H. J. Bolink, *Energy & Environmental Science*, 2014, 7, 2968-2973.
17. L. K. Ono, S. Wang, Y. Kato, S. R. Raga and Y. Qi, *Energy & Environmental Science*, 2014, 7, 3989-3993.
18. G. E. Eperon, D. Bryant, J. Troughton, S. D. Stranks, M. B. Johnston, T. Watson, D. A. Worsley and H. J. Snaith, *The Journal of Physical Chemistry Letters*, 2015, 6, 129-138.
19. C. G. Granqvist, A. Azens, P. Heszler, L. Kish and L. Österlund, *Solar Energy Materials and Solar Cells*, 2007, 91, 355-365.
20. A. Cannavale, F. Fiorito, D. Resta and G. Gigli, *Energy and Buildings*, 2013, 65, 137-145.
21. R. D. Rauh, *Electrochimica acta*, 1999, 44, 3165-3176.
22. R. Baetens, B. P. Jelle and A. Gustavsen, *Solar Energy Materials and Solar Cells*, 2010, 94, 87-105.
23. C. Bechinger, S. Ferrere, A. Zaban, J. Sprague and B. A. Gregg, *Nature*, 1996, 383, 608-610.
24. U. O. Krašovec, A. Georg, A. Georg, V. Wittwer, J. Luther and M. Topič, *Solar Energy Materials and Solar Cells*, 2004, 84, 369-380.
25. A. Georg and U. O. Krašovec, *Thin Solid Films*, 2006, 502, 246-251.
26. J.-J. Wu, M.-D. Hsieh, W.-P. Liao, W.-T. Wu and J.-S. Chen, *Acs Nano*, 2009, 3, 2297-2303.

27. A. Cannavale, M. Manca, F. Malara, L. De Marco, R. Cingolani and G. Gigli, *Energy & Environmental Science*, 2011, 4, 2567-2574.
28. A. Cannavale, M. Manca, L. De Marco, R. Grisorio, S. Carallo, G. P. Suranna and G. Gigli, *ACS applied materials & interfaces*, 2014, 6, 2415-2422.
29. A. L. Dyer, R. H. Bulloch, Y. Zhou, B. Kippelen, J. R. Reynolds and F. Zhang, *Advanced Materials*, 2014, 26, 4895-4900.
30. A. Abate, A. Petrozza, V. Roiati, S. Guarnera, H. Snaith, F. Matteucci, G. Lanzani, P. Metrangolo and G. Resnati, *Organic Electronics*, 2012, 13, 2474-2478.
31. A. Abate, A. Petrozza, G. Cavallo, G. Lanzani, F. Matteucci, D. W. Bruce, N. Houbenov, P. Metrangolo and G. Resnati, *Journal of Materials Chemistry A*, 2013, 1, 6572-6578.
32. M.-C. Yang, H.-W. Cho and J.-J. Wu, *Nanoscale*, 2014, 6, 9541-9544.
33. C. G. Granqvist, *Thin Solid Films*, 2014, 564, 1-38.
34. M. J. Reddy, J. S. Kumar, U. S. Rao and P. P. Chu, *Solid state ionics*, 2006, 177, 253-256.
35. Z. Jia, W. Yuan, H. Zhao, H. Hu and G. L. Baker, *RSC Advances*, 2014, 4, 41087-41098.
36. R. Hunt and M. Pointer, *Color Research & Application*, 1985, 10, 165-179.
37. H. J. Snaith, A. Abate, J. M. Ball, G. E. Eperon, T. Leijtens, N. K. Noel, S. D. Stranks, J. T.-W. Wang, K. Wojciechowski and W. Zhang, *The Journal of Physical Chemistry Letters*, 2014, 5, 1511-1515.